Biomass Conversion and Biorefinery
https://doi.org/10.1007/s13399-023-04008-z

ORIGINAL ARTICLE

Green synthesis of nanohydroxy apatite using *Calotropis procera* and *Wrightia tinctoria* plant latex serum extract for biomedical application

M. Suba Sri[1] · M. Subhashini[2] · M. Kalpana Devi[1] · R. Jayakala Devi[1] · R. Usha[1]

Received: 30 December 2022 / Revised: 21 February 2023 / Accepted: 27 February 2023
© The Author(s), under exclusive licence to Springer-Verlag GmbH Germany, part of Springer Nature 2023

Abstract
Medical textiles have become increasingly important and extend the strong protection role in the healthcare industry. The goal of this study was to improve conventional cotton gauze into advanced biomedical specifications with antimicrobial activity. The cotton gauze fabrics were modified by in situ wet chemical precipitation of hydroxyapatite nanoparticles (HAp NP) with *Calotropis procera* and *Wrightia tinctoria* plant latex serum extract. The developed nanoparticles were initially examined by UV–visible spectrophotometer with maximum absorbance peak at 274 nm for *Calotropis procera* and 286 nm for *Wrightia tinctoria*. To determine the lattice formation and average crystal size, X-ray diffraction (XRD) study was done and the size was observed as 31.13 µm and 29.18 µm for *Calotropis procera* and *Wrightia tinctoria* serum extract hydroxyapatite nanoparticles respectively. Fourier transform infra-red spectroscopy (FTIR) confirmed the presence of functional groups such as the carbonate and phosphate group in both the developed nanoparticle as they are the important agents for forming Hap. The scanning electron microscope (SEM) result confirms the developed nanoparticle was hexagonal in shape with polycrystalline morphology. Deposition of *Calotropis procera* and *Wrightia tinctoria* HAp NP onto cotton gauze fabrics resulted in significant antimicrobial activity with zone of inhibition against *Candida albicans*, *Aspergillus niger*, *Staphylococcus aureus*, and *Escherichia coli*. Hence, the present work highlighted the development of plant extract-mediated hydroxyapatite nanoparticles having excellent antibacterial properties and it can be recommended for medical application.

Keywords Hydroxyapatite nanoparticle · Plant latex serum · X-ray diffraction · UV–visible spectrophotometer · FTIR and SEM

1 Introduction

Nanoscience is one of the most interesting prospects in nanotechnology, as it enhances design and function while introducing novel features. Because of their enhanced surface area and quantum confinement effects, nanotechnology offers a unique way to address the shortcomings of bulk materials [1]. Polymers, ceramics, and metals can all be used to make nanoparticles. Nanomaterials are different from nanoparticles in that they have distinct qualities and applications derived from their features, and they can be used to make Nano finished materials. Ceramic nanoparticles are the most recent trend in nanomaterials, owing to their high yield strength and low density. Roy and coworkers reported that the ceramic-based nanoparticles can be used as photodynamic therapy for treating cancer and bone tissue engineering. The future implication of nanotechnology aids in the creation of many new materials and devices with vast range of applications in the fields of nano-medicine, nano-electronics, and biomaterials [2].

Hydroxyapatite [$Ca_{10}(PO_4)_6(OH)_2$] is a naturally occurring mineral form of calcium apatite. Since hydroxyapatite is a modified form of human bone with 50% volume and 70% weight, it is referred to as a bone mineral. For the past 40 years, bone deficiency and tissue disease have been significant health issues, and ceramic-based biomaterials have been created to enhance treatment [3]. Transplantation and implantation are the two ways for replacing the

✉ R. Usha
ushaanbu09@gmail.com

[1] Department of Microbiology, Karpagam Academy of Higher Education, Coimbatore, Tamil Nadu, India

[2] Department of Microbiology, PSG College of Arts and Science, Coimbatore, Tamil Nadu, India

Published online: 13 April 2023

tissue. Bioinert and bioactive ceramic are the two classified groups in bio ceramic. Hydroxyapatite has been perceived as a bone substitute material in dentistry and orthopedics. Hydroxyapatite is a well-known biomaterial because of its excellent bioactivity, biocompatibility, and osteoconductivity [4]. Hydroxyapatite can be utilized to treat bone deformities, as a tissue scaffold, as a covering on metallic implants, and as a drug delivery carrier [5]. In bone tissue engineering, the development of biomaterials made of hydroxyapatite and antibiotics is highly effective for filling bone deficiencies [6]. The hydroxyapatite nanoparticles synthesized by biological methods offer immense advantages and remarkable attention because of their unique properties [19]. Calcium and phosphate salt in aqueous solution were used to create hydroxyapatite nanoparticles. The aggregation of particles in hydroxyapatite produced by wet chemical precipitation in aqueous solution has a drawback. To stop the aggregation of hydroxyapatite nanoparticles, natural rubber latex has been developed as a templating agent in place of aqueous solution [7]. The crystal structure of hydroxyapatite are mostly hexagonal in shape in which it consists of two types of Ca sites and nine oxygen atoms in the first site which forms polyhedron and the five oxygen atoms and one hydroxyl groups in the second site which forms octahedron [20].

In the current research, hydroxyapatite nanoparticle production used serum from latex-producing plants as a solvent. Secondary metabolites found in the latex-producing plants' serum serve as a template for the creation of the nanoparticles. The bioactive and therapeutic substances found in plant latex serum can be used to create hydroxyapatite nanoparticles, which has two benefits. One advantage is that it can overcome the agglomeration of particles which can be used for drug delivery. Another advantage is the availability of medicinal chemicals in latex plant serum, which can be used to make hydroxyapatite nanoparticles for biomedical applications. *Calotropis procera* and *Wrightia tinctoria*, two latex-producing plants often found in India, are adaptable plants with immense medical value. Generally, latex consists of three components such as rubber, serum, and lipid. Serum fractions of the plants contain phytocompounds which has higher medicinal values for treating various diseases [8]. *Calotropis procera* belongs to *Asclepiadaceae* family belongs to subfamily Apocynaceae. Latex produced from the plant arise from a branching tubes present in the stem which exhibits diverse curative properties [9]. The latex serum of the plant contains protein including antioxidant enzymes which has radical scavenging activity. *Wrightia tinctoria* is an ancient medicinal plant belongs to *Apocynaceae* family. Latex of the plant is used as a painkiller and has wound healing activity folk medicine. The plant has antioxidant, anti-inflammatory, antimicrobial, anti-diabetic, anti-ulcer, and anti-psoriatic activity. The aforementioned two plants were chosen for biosynthesis because they contain a variety of bioactive components such as alkaloids, flavonoids, terpenoids, tannins, phenolic compounds, carbohydrates, and proteins, among other things. Plant latex serum is used as a solvent in this study to create hydroxyapatite nanoparticles. Hydroxyapatite can be made in a variety of ways, including dry and wet synthesis. Dry synthesis takes a lengthy time and uses a high temperature, whereas wet synthesis uses a low temperature and produces nanoparticles quickly [10]. Hydroxyapatite is an ideal candidate for biomedical applications and possesses gold standard in medical sector such as to develop artificial teeth and bone which is similar to human to make excellent nanocomposites and nanomaterials. In the present work, the latex serum extract-mediated nanohydroxyapatite was characterized and coated in cotton gauze for determining the antimicrobial activity. Hence, HAp Nps can be used as a bio-vehicle for drug delivery since they have affinity to DNA, proteins, and various drugs with proper drug release [22]. The present research suggests that physical and chemical characterization and antimicrobial activity of the developed HAp Nps have multidisciplinary biological application as an advanced biomaterial in the field of bio-therapeutics.

2 Materials and method

2.1 Collection and fractionation of latex from plants

Calotropis procera and *Wrightia tinctoria* crude latex were collected separately in distilled water (1:1) and centrifuged for 10 min at 5000 rpm at 4 °C to separate the water insoluble rubber, lipid precipitate, and serum. The serum-containing supernatant from the aqueous fraction was collected and kept for nanoparticle synthesis [11].

2.2 Phytochemical analysis of latex serum extracts

Calotropis procera and *Wrightia tinctoria* serum fractions were separated and screened for alkaloids, phenolic compounds, flavonoids, terpenoids, tannins, saponins, resins, cardiac glycosides, and proteins [12].

2.3 Production of hydroxyapatite nanoparticle by the wet chemical precipitation method

About 0.55 g of calcium chloride was mixed with 5-ml serum of *Calotropis procera* and *Wrightia tinctoria* was taken separately and maintained at pH 10 by using 0.8 M sodium hydroxide. Similarly, 0.425 g of disodium hydrogen phosphate also used along with plant serum. and stirred vigorously. To the stirring mixture, serum-containing disodium hydrogen phosphate was added in drops and observed for the formation of gelatinous white precipitate. The reaction

mixture was then stirred in a magnetic stirrer for 1 h at room temperature and kept 24 h for aging. The resultant precipitate was then washed many times with distilled water until the pH was neutral to get *Calotropis procera* serum and *Wrightia tinctoria* serum hydroxyapatite nanoparticle in solution form. The obtained HAp precipitate was dried in hot air oven at 60 °C for 12 h to get powder form. Similarly, control was maintained using distilled water [4].

2.4 UV–visible spectrophotometer characterization of developed hydroxyapatite nanoparticle

UV–Vis spectroscopy was used to examine the generated hydroxyapatite nanoparticles from two latex serum extracts. By drawing 1 cm^3 of the samples in the Eppendorf UV–Vis spectrophotometer (Eppendorf, India), the spectrum was recorded in the wavelength range of 200–700 nm. All of the developed hydroxyapatite nanoparticles had their absorbance and plasmon peak measured [13].

2.5 Fourier transform infra-red spectroscopy characterization of developed hydroxyapatite nanoparticle

A Shimadzu-single reflection ATR auxiliary Fourier transform infra-red spectrometer (Shimadzu, India) was used to detect the existence of functional groups and chemical bonds in the generated hydroxyapatite nanoparticle from two distinct latex serum extracts (FTIR). The spectrum was found to be in the 400–4000 cm^{-1} range [14].

2.6 X-ray diffraction characterization of developed hydroxyapatite nanoparticle

Using an X-ray diffractometer (Shimadzu, India), with Cu K monochromatic radiation (1.5406) as a source in the range of 0 280, the produced hydroxyapatite nanoparticles from two different latex serum extracts were examined. The developed hydroxyapatite nanoparticle from *Calotropis procera* and *Wrightia tinctoria* serum, as well as a control using double distilled water in solution form, were centrifuged separately at a speed of 2000 RPM. The pellet was then dried in a water bath at 60 °C for 30–40 min before being crushed to make fine powders for XRD analysis [4].

The following equation was used to compute the lattice parameters (a and c) of a produced hydroxyapatite nanoparticle.

$$1/\mathbf{d}2 = 4(\mathbf{h}2 + \mathbf{hk} + \mathbf{k}2)/3\mathbf{a}2 + \mathbf{l}2/\mathbf{c}2 \quad (1)$$

The interplanar gap between the atomic lattices is denoted by d. The volume V of the hexagonal unit cell formed by produced hydroxyapatite nanoparticles was determined using the equation below.

$$\mathbf{V} = \sqrt{3/2} * \mathbf{a}^2 * \mathbf{C} \quad (2)$$

Using the Debye-Scherrer equation, the crystallite size of produced hydroxyapatite nanoparticles along the c-axis was estimated from the XRD pattern.

$$\mathbf{Dhkl} = \mathbf{K}\lambda/\beta 1/2\ \mathbf{cos}\theta \quad (3)$$

where Dhkl is the crystallite size, K is the Debye-Scherrer constant, is the wavelength of Cu K radiation (1.5406), 1/2 is the FWHM (full width at half maximum) of the (111) peak (in radian), and is the diffraction angle (in degrees).

2.7 Development of hydroxyapatite nanoparticle-coated gauze

A fine 100% cotton gauze samples (30×30 cm^2) were used for the application study. HAp NPs applied on gauze material using the pad-dry-cure-method. The gauze material was immersed nanoparticle for 10 min; then, it was passed through the padding mangle. After padding, the fabric was air-dried at room temperature [15].

2.8 Topographical analysis of nanoparticle-coated medical gauze by SEM

The prepared samples morphology and elemental composition were examined using scanning electron microscopy (SEM) at accelerating voltage 20 kV. The length of 3*3 cm was taken from the control and two latex serum extract hydroxyapatite nanoparticle and topographic analysis was performed using scanning electron microscope.

2.9 Antimicrobial activity of the developed nanoparticle-coated gauze

The agar disk diffusion technique was used to investigate the antimicrobial activities. In nutrient agar plates, *S. aureus*, *E. coli*, and the fungi *Candida albicans* and *Aspergillus niger* were inoculated (0.1 mL of 10^5–10^6 cells/mL). The cotton gauze samples were then placed on top of the agar, and the plates were left at 4 °C for 2–4 h to allow the antimicrobial compounds to disperse. Plates were then moved to 37 °C for 24 h for bacteria and 30 °C for 48 h for fungi. The diameter of the growth inhibition zone was used to determine the antimicrobial activity of the sample (in mm). The data consisted of the mean values of several independent experiments.

2.10 Mechanical strength of the developed hydroxyapatite nanoparticle-coated gauze

The tensile properties of the developed hydroxyapatite nanoparticle were analyzed by Zwick-Roell testing machine at a crosshead speed of 5 mm/min. The thickness of the developed hydroxyapatite nanoparticle was determined using the thickness gage Tilmet (ASTM D 1777-96). The rectangular sample was 10 cm long and 2 cm wide and was taken for analysis to determine the mean breaking strength, mean breaking elongation, and stress/strain percentage [7].

2.11 Toxicity analysis of the developed nanoparticle by MTT assay

Cell viability and cytotoxicity assays were performed to find the cytotoxicity of the developed hydroxyapatite nanoparticle. The Dulbecco's Modified Eagle Medium (DMEM) comprises of 0.195 g, Glucose 0.045 g, Sodium carbonate 0.037 g was prepared in 10-ml T Flask. To this medium, L 929 fibroblast cell line was inoculated. The media was incubated at 37 °C/24 h. The test dilution 25, 50, 75, and 100 µl of developed *Calotropis procera* and *Wrightia tinctoria* hydroxyapatite nanoparticle were added along with cell line 500 µl and dye 500 µl [18].

3 results and discussion

3.1 Fractionation of plant latex

The collected latex from the plants was fractioned for serum separation and stored in a refrigerator at 4 °C for future use. Figure 1 represents the fractionation of rubber, serum, and lipids from the latex serum extract. The serum fraction in the middle layer can be pipetted out for further analysis without disturbing the solid rubber and lipid. The natural rubber latex of *Calotropis procera* can be separated by centrifugation for 20 min at 4 °C; 3 layers were formed in which clear middle fraction of serum contain many bioactive compounds [21].

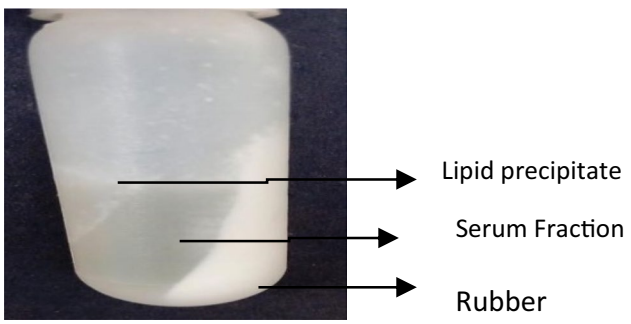

Fig. 1 Fractionation of latex serum extract

Table 1 Phytochemical analysis of *Calotropis procera* and *Wrightia tinctoria* latex serum extract

Phytoconstituents	Aqueous extract of *Calotropis procera*	Aqueous extract of *Wrightia tinctoria*
Alkaloids	+	+
Phenolic compounds	−	+
Flavonoids	+	+
Terpenes	+	+
Tannins	+	−
Saponins	+	−
Resins	+	−
Glycosides	+	−
Proteins	+	+

3.2 Phytochemical analysis of latex serum extracts

The phytochemical contents contained in the latex serum of *Calotropis procera* and *Wrightia tinctoria* were investigated using standard techniques, and the results are presented in Table 1. The presence of alkaloids, flavanoids, and proteins was determined by phytochemical screening of all of the plants. Phenolic chemical was absent in *Calotropis procera*. Terpenes and tannins are present in *Wrightia tinctoria. Calotropis procera* contained resins and glycosides, whereas glycosides are absent in *Wrightia tinctoria*. The phytochemical analysis of aqueous extract of *Calotropis procera* indicates the presence of saponins, tannins, resins, glycosides, and flavanoids [12]. *Wrightia tinctoria* extracts preliminary phytochemical analysis reveals the presence of flavonoids, phenolic compounds, steroids, and tannins [16].

3.3 Production of hydroxyapatite nanoparticle by the wet chemical precipitation method

The wet chemical precipitation method was adopted to make hydroxyapatite nanoparticles from latex serum extracts of *Calotropis procera* and *Wrightia tinctoria* in which the serum extracts act as a templating agent and calcium phosphate and disodium hydrogen phosphate act as a precursors for the synthesizing of HAp Nps. White precipitate was formed after 24 h of the stirring process. Air-dried powder was obtained after 12 h. Figure 2 shows the formation of hydroxyapatite nanoparticles using a wet chemical precipitation process. Similarly, Govindan et al. (2017) produced hydroxyapatite nanoparticle using *Azadirachta indica* and *Coccinia grandis* with calcium chloride and disodium hydrogen phosphate as a precursors and air-dried powder was obtained [4]. The hydroxyapatite nanoparticle produced from calcium nitrate tetrahydrate and diammonium hydrogen phosphate as a precursors yield hydroxyapatite nanoparticle in the solution phase [17].

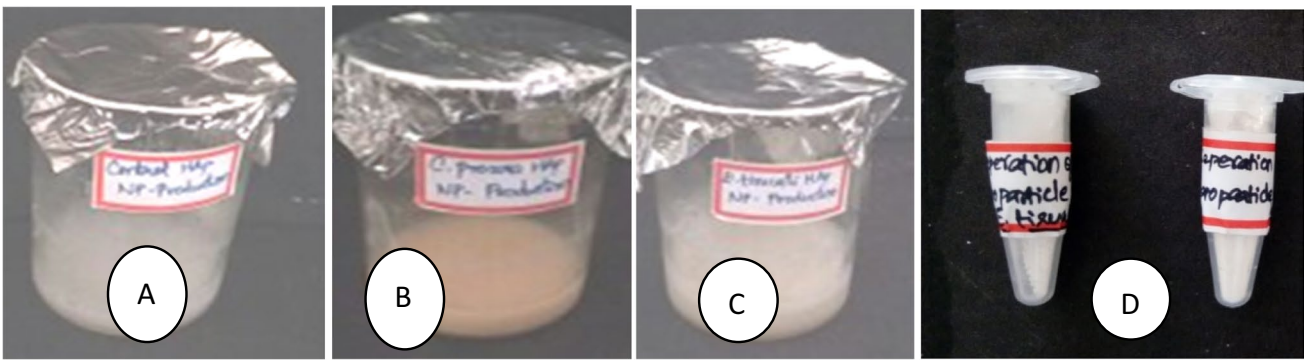

Fig. 2 Production of hydroxyapatite nanoparticle by wet chemical precipitation method (**A** control, **B** *Calotropis procera* serum nanoparticle, **C** *Wrightia tinctoria* serum nanoparticle, **D** dry powder of plant serum nanoparticle)

3.4 UV–visible spectrophotometer characterization of developed hydroxyapatite nanoparticle

A UV–visible spectrophotometer was used to characterize the produced hydroxyapatite nanoparticle in solution form. The spectrum was captured at wavelengths ranging from 200 to 600 nm. For control, a maximum absorbance of 0.840 was observed at a wavelength of 259 nm (Fig. 3a). Figure 3b shows the UV–visible measurement of generated hydroxyapatite nanoparticles utilizing *Calotropis procera* latex serum extract, with an absorbance of 1.915 at 274 nm. The UV–visible examination of produced hydroxyapatite nanoparticles employing *Wrightia tinctoria* latex serum extracts and 2.349 absorbance at wavelength 273 nm is shown in Fig. 3c. Surface plasmon effect is due to the formation of calcium apatite in the serum extract of plants; hence, the maximum absorbance was obtained. Similarly, in the UV–Vis spectra of hydroxyapatite nanoparticles with polyethylene glycol and folic acid, absorption was observed at wavelengths of 278 nm and 272 nm respectively [13].

3.5 X-ray diffraction characterization of developed hydroxyapatite nanoparticle

The identification of texture, crystallinity, and residual stress XRD technique is essential. Furthermore, the changes in physical, chemical, and biological properties of the biomaterial can be due to their changes in crystallinity, morphology, solubility, and heat stability [23]. The small temperature and pH change during synthesis can affect the lattice parameters and differences in crystallinity may occur. Hence, the X-ray diffraction study is the foremost important to know about the synthesized hydroxyapatite nanoparticle crystallinity and lattice parameters. The presence of broad peaks in the region of 20° to 50° indicates the presence of partial nanohydroxyapatite [24]. It was demonstrated that the manufactured samples were pure hydroxyapatite with a hexagonal crystal structure by comparing the JCPDS (Joint Committee on Powder Diffraction Standards) data to the XRD patterns of created hydroxyapatite nanoparticles using control and latex serum extracts. Miller's planes of hydroxyapatite have a large peak in the 30–34 range, which was derived from plant latex serum extract and controls (111), (101), and (102). The resolution of the peak is determined by crystallite production and crystalline composition. The hydroxyapatite nanoparticle in latex serum extract produced the broad diffraction peak (samples). The generated hydroxyapatite nanoparticle's X-ray diffraction analysis with lattice constant, unit cell volume, and average crystallite size is shown in Table 2. The XRD analysis of control hydroxyapatite is shown in Fig. 4a, the XRD analysis of developed hydroxyapatite nanoparticle using *Calotropis procera* latex serum extract is shown in Fig. 4b, and the XRD analysis of developed hydroxyapatite nanoparticle using *Wrightia tinctoria* latex serum extract is shown in Fig. 4c. The sharp, high-intensity peak at angles 25.9 and 31.8, with miller indices (hkl values) of (002) and (211), respectively corresponded to HAp crystals. The hexagonal structure of HAp crystals was revealed by XRD analysis (PDF card number 009–0432 and 01–072-1243). Small crystallites of about 5 nm were used to create HAp crystals (the crystallite size was calculated using the Scherrer formula). The diffraction peaks at 16.5 and 22.8 vanished as the HAp concentration increased. The 47.1 peak corresponded to HAp (222) lattice planes. The strong crystallinity of hydroxyapatite nanoparticles is indicated by the intense peak at 31.8, which causes narrow peaks in the diffractogram [18]. Similarly, the standard data of hydroxyapatite (HAp) powder (JCPDS090432) was equivalent to the manufactured hydroxyapatite samples with Miller planes such as (002), (211), (300), and (310) correspondingly [7].

3.6 Fourier transform infra-red spectroscopy characterization of developed hydroxyapatite nanoparticle

FTIR analysis represents the biomolecules and functional groups present in the Hydroxy apatite nanoparticle produced from serum extract of four latex-producing plants.

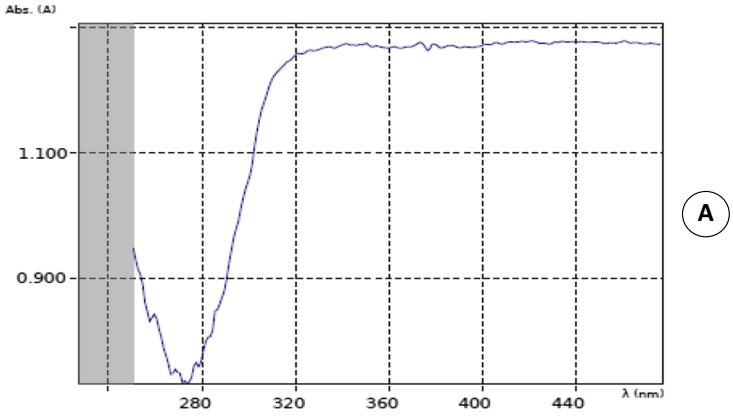

13:33 #001

Peaks:	Peak width (nm):	4
	Peak height (A):	0.020
	Wavelength (nm)	Absorbance (A)
	259	0.840

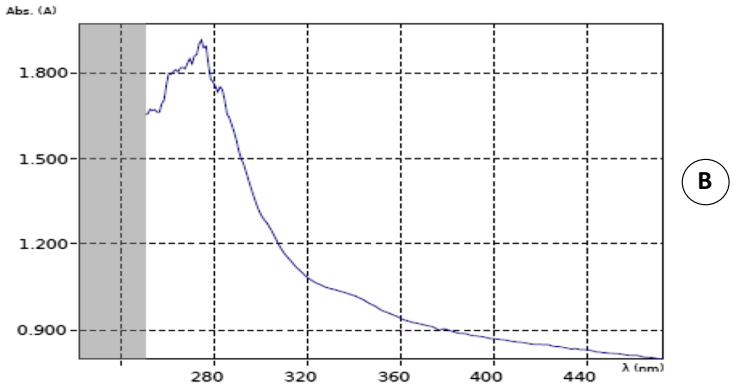

13:52 #001

Peaks:	Peak width (nm):	7
	Peak height (A):	0.020
	Wavelength (nm)	Absorbance (A)
	274	1.915

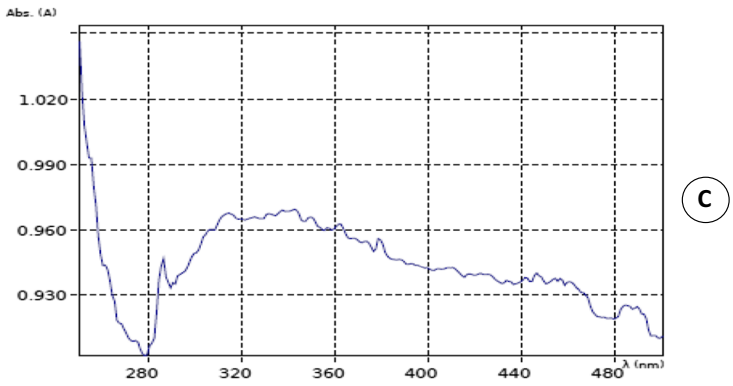

14:07 #001

Peaks:	Peak width (nm):	7
	Peak height (A):	0.020
	Wavelength (nm)	Absorbance (A)
	286	0.947

Fig. 3 UV–Visible analysis of control (**A**), *Calotropis procera* hydroxyapatite nanoparticle (**B**), *Wrightia tinctoria* hydroxyapatite nanoparticle (**C**)

Table 2 XRD analysis of developed hydroxyapatite nanoparticle (1, control; 2, *Calotropis procera Hap*; *3*, *Wrightia tinctoria hap*)

Sample	Peak (theta degree)	Lattice constant (Å) a = b	Lattice constant (Å) C	Unit cell volume V(Å^3)	Average crystallite size D
1	32	12.87	9.24	1325.43	25.62
2	32	14.144	9.32	1614.69	31.13
3	32	12.64	9.19	1271.57	29.18

FTIR is an important characterization for hydroxyapatite nanoparticle because the presence of carbonate group is very essential as the human bone contains 4–6% of carbonate weight [22]. The presence of the carbonate and phosphate group in the serum extract HAp Np were represented in Table 3 and Fig. 5; hence, this is the indication of hydroxyapatite nanoparticle formation. Table 3 represents the FTIR analysis of developed hydroxyapatite nanoparticle from latex serum extract and control. The alcoholic group, carbonate group, and phosphate group are the most important functional groups which must be present in the hydroxyapatite nanoparticle. The FTIR analysis of the generated control hydroxyapatite nanoparticle is depicted in Fig. 5a. Alcoholic (OH) functional groups are shown by prominent and broad peaks at 3541.31 cm^{-1}. The presence of the carbonate group was confirmed by the presence of a peak at 1442.75 cm^{-1} and 871.82 cm^{-1} for control, and the presence of the phosphate group was confirmed by the presence of a peak at 1064.71 cm^{-1} and 570.93 cm^{-1}. The FTIR analysis of generated hydroxyapatite nanoparticles employing *Calotropis procera* latex serum extract is represented in Fig. 5b. The presence of the alcohol group was indicated by a wide peak at 3471.87 cm^{-1}. The carbonate group was represented by peaks at 1419.61 cm^{-1} and 864.11 cm^{-1}, whereas the phosphate group was validated by hydroxyapatite peaks at 1072.42 cm^{-1} and 586.36 cm^{-1}. The findings of the FTIR examination of generated hydroxyapatite nanoparticles employing *Wrightia tinctoria* latex serum extract are shown in Fig. 5c. The presence of a peak at 3541.31 cm^{-1} indicated the presence of an alcoholic functional group. The presence of carbonate group was confirmed by the presence of peak at 1458.18 cm^{-1} and 871.82 cm^{-1} for hydroxyapatite nanoparticle developed from *Wrightia tinctoria* latex serum extract, and the phosphate group was confirmed by the presence of peak at 1041.56 cm^{-1} and 524.64 cm^{-1} for hydroxyapatite nanoparticle developed from *Wrightia tinctoria* latex serum extract. The absorption band at 3571 cm^{-1} attribute to the presence of alcohol functional group and the peak at 1457 cm^{-1}, 1414 cm^{-1}, and 1457 cm^{-1} were the main characteristic for hydroxyapatite nanoparticle which belongs to carbonate group [3]. Similarly, FTIR spectrum of hydroxyapatite nanoparticle shows vibrational modes of peak at 462 cm^{-1}, 565 cm^{-1}, 605 cm^{-1}, 961 cm^{-1}, 1032 cm^{-1}, and 1108 cm^{-1} represents the presence of the phosphate group and the peaks at 3569 cm^{-1} indicates the presence of the alcohol group [5].

3.7 Topographical analysis of developed nanoparticle-coated medical gauze by scanning electron microscopy

Scanning electron microscope was used to examine the morphological appearance and particle size of the produced hydroxyapatite nanoparticle (SEM). Rod-like hydroxyapatite Nps were considered because of the similarity to rod-like nanocrystalline structures present in natural human bone [25]. The produced hydroxyapatite nanoparticle was aggregated, as evidenced by the SEM pictures at 200X, 750X, 2000X, and 5000X magnifications. The produced hydroxyapatite nanoparticles were analyzed in the micrographs in the size range of 2–100 µm with a variety of shape. The highest concentration of calcium apatite and phosphate formation was observed in the serum extract nanoparticle than the control in SEM data which shows crystal morphology. The deposition of plant HAp NPs on cotton gauze will increase as a result of the HAp NPs (negatively charged) coating when compared to unmodified cotton gauze. Plant latex serum extract can act as an excellent chelating agent, stabilizer, and reducing agent for the formation of HAp NPs and protecting them from agglomeration due to the chelating functional groups (-NH_2 and -OH) in its structure. Figure 6a showed SEM pictures of control hydroxyapatite, while Fig. 6b showed SEM images of developed hydroxyapatite nanoparticles using *Calotropis procera* latex serum extract and Fig. 6c showed SEM photos of developed hydroxyapatite nanoparticles using *Wrightia tinctoria* latex serum extract. The hydroxyapatite samples were agglomerated due to the gel formation in primary drying and observed as nanorods [18, 19]. Similarly, the hydroxyapatite nanoparticle was needle in shape with particle size 82.63 nm at 700 °C production temperature [3].

3.8 Antimicrobial activity of the developed nanoparticle-coated gauze

The development of protective fabrics is critical for many applications, particularly in the medical field. The nano-size of the developed hydroxyapatite has reliable surface contact area with the microbial cells, and hence, there is a better interaction that took place to inhibit the microbial cell wall. The antimicrobial activities of various cotton gauze samples were determined using the qualitative (inhibition zone) method against *S. aureus*, *E. coli*, and the fungi *C. Albicans* and *A. niger*. The

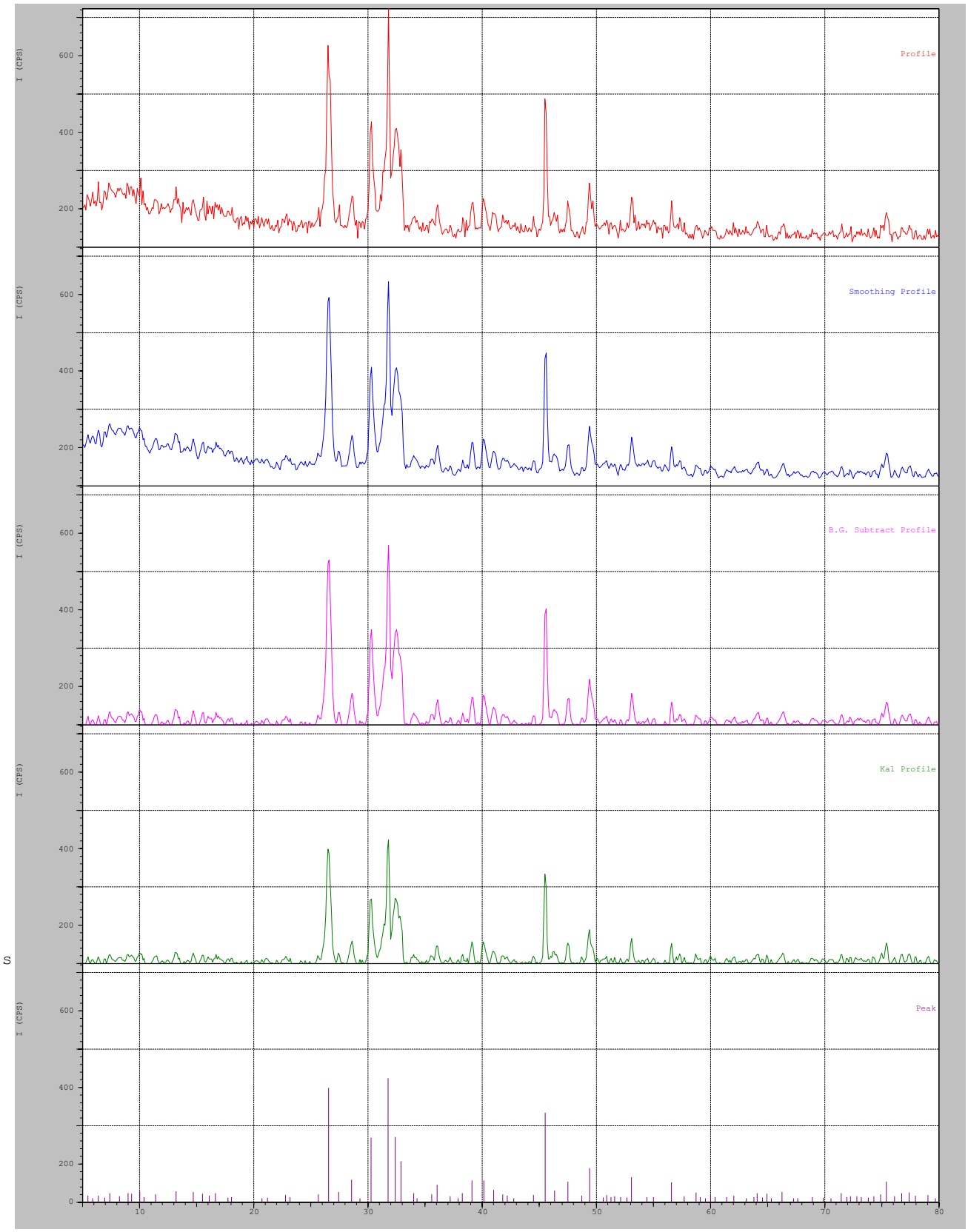

Fig. 4 **A** X-ray diffraction analysis of control hydroxyapatite nanoparticle. **B** XRD analysis of hydroxyapatite nanoparticle developed from *Calotropis procera* latex serum extract. **C** XRD analysis of hydroxyapatite nanoparticle developed from *Wrightia tinctoria* latex serum extract

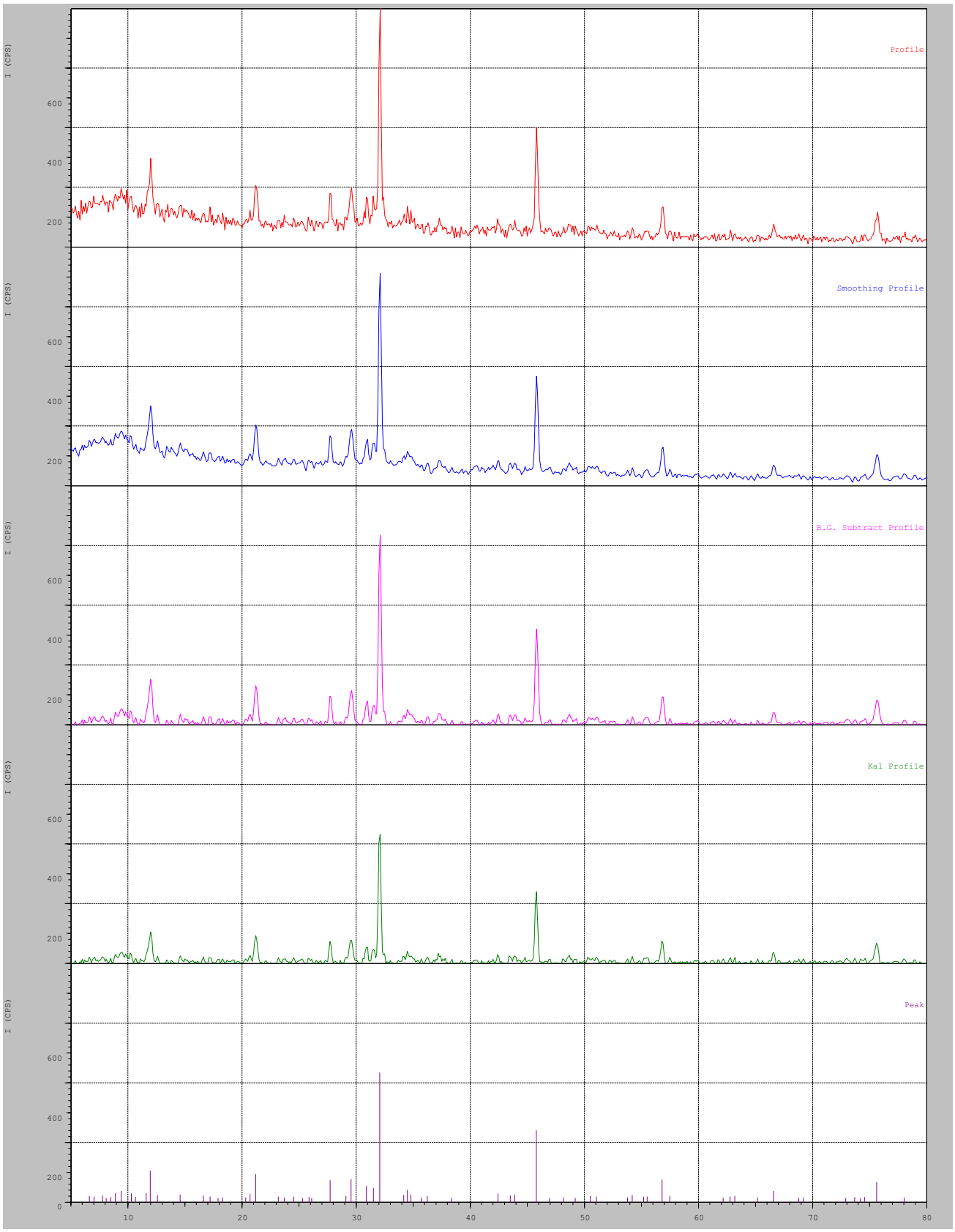

Fig. 4 (continued)

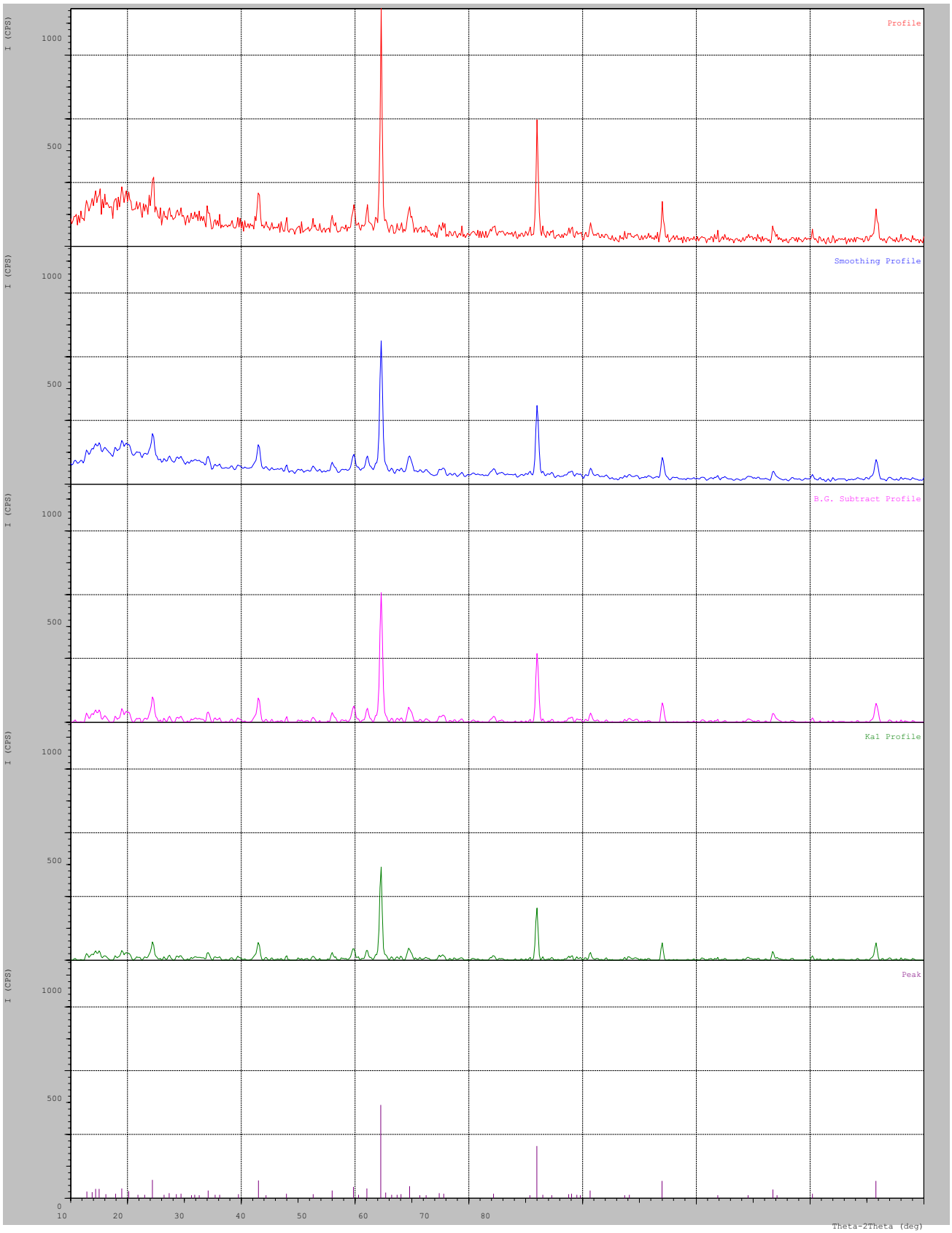

Fig. 4 (continued)

Table 3 FTIR analysis of developed hydroxyapatite nanoparticle (1, control; 2, *Calotropis procera Hap*; *3*, *Wrightia tinctoria hap*)

S. No	Control peaks (cm^{-1})	*Calotropis procera* peaks (cm^{-1})	*Wrightia tinctoria* peaks (cm^{-1})	Functional groups
1	1442.75 & 871.82	1419.61 & 864.11	1458.18 & 871.82	CO3 (carbonate group)
2	1064.71 & 570.93	1072.42 & 586.36	1041.56 & 524.64	PO4 (phosphate group)
3	3541.31	3471.87	3541.31	OH (alcohol group)

Presence of functional groups such as carbonate, phosphate and alcohol group in control and plant latex serum hydroxyapatite nanoparticle were tabulated

absence of the inhibition zone indicated that the unmodified (control) cotton gauze had no antimicrobial activity against the tested microorganisms (Table 4). In contrast, the incorporation of HAp NPs in the samples resulted in good antimicrobial performance (i.e., the presence of the inhibition zone) against *E. coli* (highest effect), *S. aureus*, and C. *albicans*, but not *A. niger*. HAp-doped nanoparticles have recently attracted a lot of attention. The HAp has strong antibacterial activity because the electrostatic force attracts bacterial cells to the surface of the HAp, where there is a direct interaction between the bacterial cell membrane and the calcium and phosphate ions present in hydroxyapatite [17]. This study findings confirm that radicals were responsible for the antibacterial properties. Other studies have found that HAp NP has antimicrobial activity against a variety of microorganisms. This property could be explained by a number of factors, the most important of which are HAp NP dissolution and the release of plant serum extract. Through electrostatic attractions, the plant serum extract can interact with the negatively charged microbe membrane, inhibiting their growth. Furthermore, plant-mediated HAp ions can interact with the -SH groups of microbe enzymes, inhibiting them. Plant latex serum extract can also enter microorganisms and damage their DNA. Our findings showed that HAp NPs incorporated into the modified samples inhibited G bacteria more effectively than G + bacteria. This is explained by the electrostatic attraction between positively charged Ca^{2+} ions and negatively charged G cell membranes, which facilitates the attachment of Ca^{2+} and PO^{4-} ions to the membrane. HAp NPs act in fungi through depletion, which causes irregularly shaped pits in the fungal outer membrane and changes membrane permeability, resulting in the release of membrane lipopolysaccharides and proteins [18].

3.9 Mechanical strength of the developed nanoparticle-coated gauze

Mean breaking strength and mean breaking elongation of the developed hydroxyapatite nanoparticle were determined along with the strain percentage. Mean breaking strength F_{max} of *Calotropis procera* and *Wrightia tinctoria* hydroxyapatite nanoparticle-coated gauze was determined as 1.43 N and 1.46 N. Mean breaking elongation dL at F_{max} of *Calotropis procera* and *Wrightia tinctoria* hydroxyapatite nanoparticle-coated gauze was determined as 22.9% and 23.0%. Similarly, Aliharli et al. (2022) reported that the nanofibrous scaffold has higher flexibility and tensile strength than the other microfibrous or hybrid scaffold developed from polyvinyl alcohol and hydroxyapatite respectively. The thickness of the developed nanoparticle-coated gauze from *Calotropis procera* and *Wrightia tinctoria* hydroxyapatite nanoparticle was determined as 0.12 mm and 0.13 mm. Similarly, Ganta et al. (2020) reported that the thickness of polyvinyl alcohol with hydroxyapatite nanofibrous scaffold was determined as 0.11 mm.

3.10 Toxicity analysis of the developed nanoparticle by MTT assay

Cell viability was assessed using this method's MTT test. The color of the L 929 fibroblast cell line changed after incubation. Numerous in vitro tests of a cell population reaction to outside influences are based on measurements of cell viability and proliferation. Tetrazolium salt reduction is now recognized as a trustworthy method for assessing cell growth. Dehydrogenase enzymes help metabolically active cells reduce the yellow tetrazolium MTT (3-(4,5-dimethyl thiazolyl-2)-2,5 diphenyl tetrazolium bromide) to produce reducing equivalents like NADH and NADPH [17]. By using spectrophotometric techniques, the resulting intracellular purple formazan was solubilized and measured. 95.6% of cells were retained after the treatment with *Calotropis procera* and 96.3 % of cells were retained after the treatment with *Wrightia tinctoria* hydroxyapatite nanoparticle while the control hydroxyapatite nanoparticle has 96.1% viability. This prepared nanoparticles were found to be non-toxic to fibroblast cell line. Similarly, Aliharli et al. (2022) reported that the bioactivity of developed hydroxyapatite nanoparticle with polyvinyl alcohol has 92 % viable cells. The growth of MTT cells assay quantifies the rate of cell division when metabolic processes result in apoptosis or necrosis, the assay assesses the rate of cell growth and conversely, the decline in cell viability [12]. To speed up sample processing, as few assay steps as possible have been used. The MTT assay produces low background absorbance levels when cells are absent. The linear link between cell number and signal production is established for each kind of cell, enabling precise measurement of changes in the rate of cell proliferation [18].

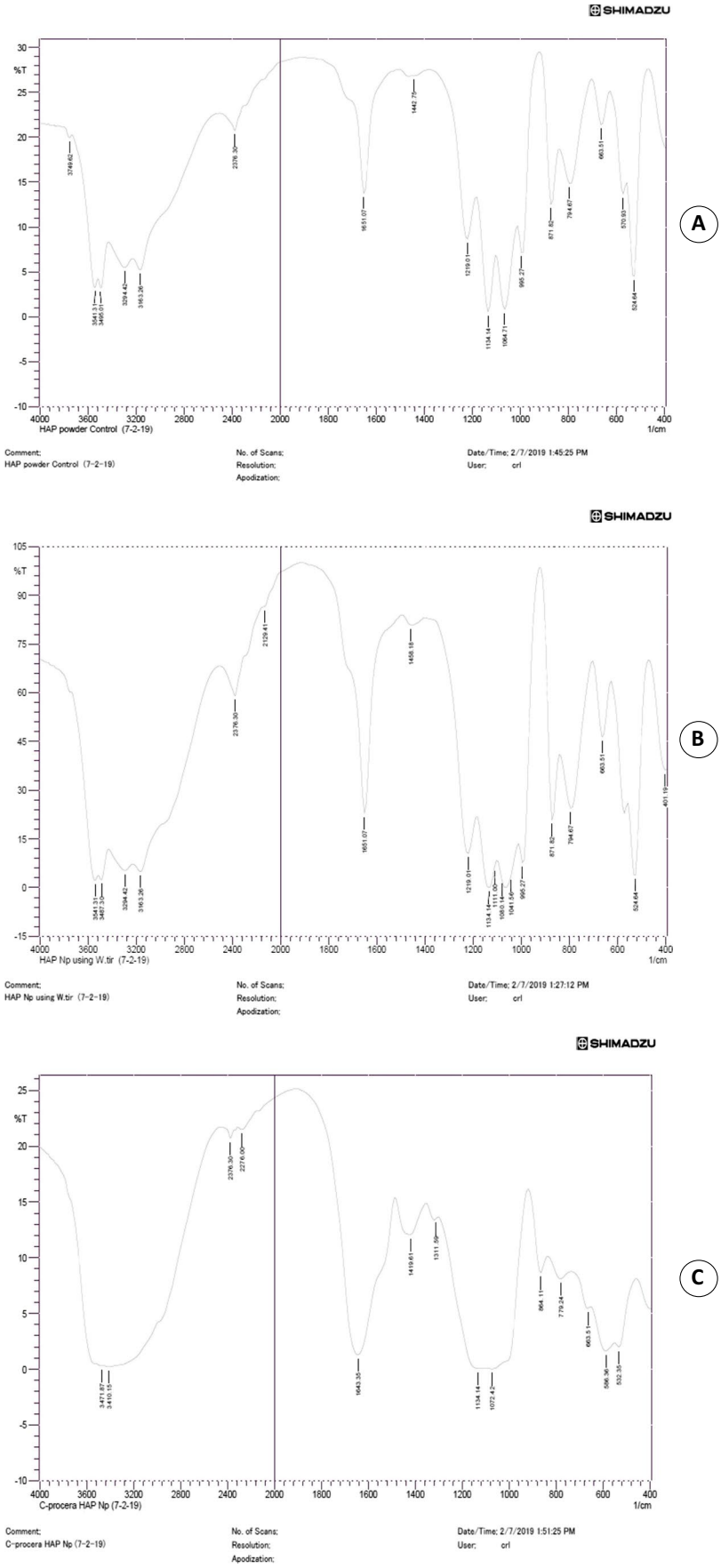

Fig. 5 FTIR analysis of control (**A**), *Calotropis procera* hydroxyapatite nanoparticle (**B**), *Wrightia tinctoria* hydroxyapatite nanoparticle (**C**)

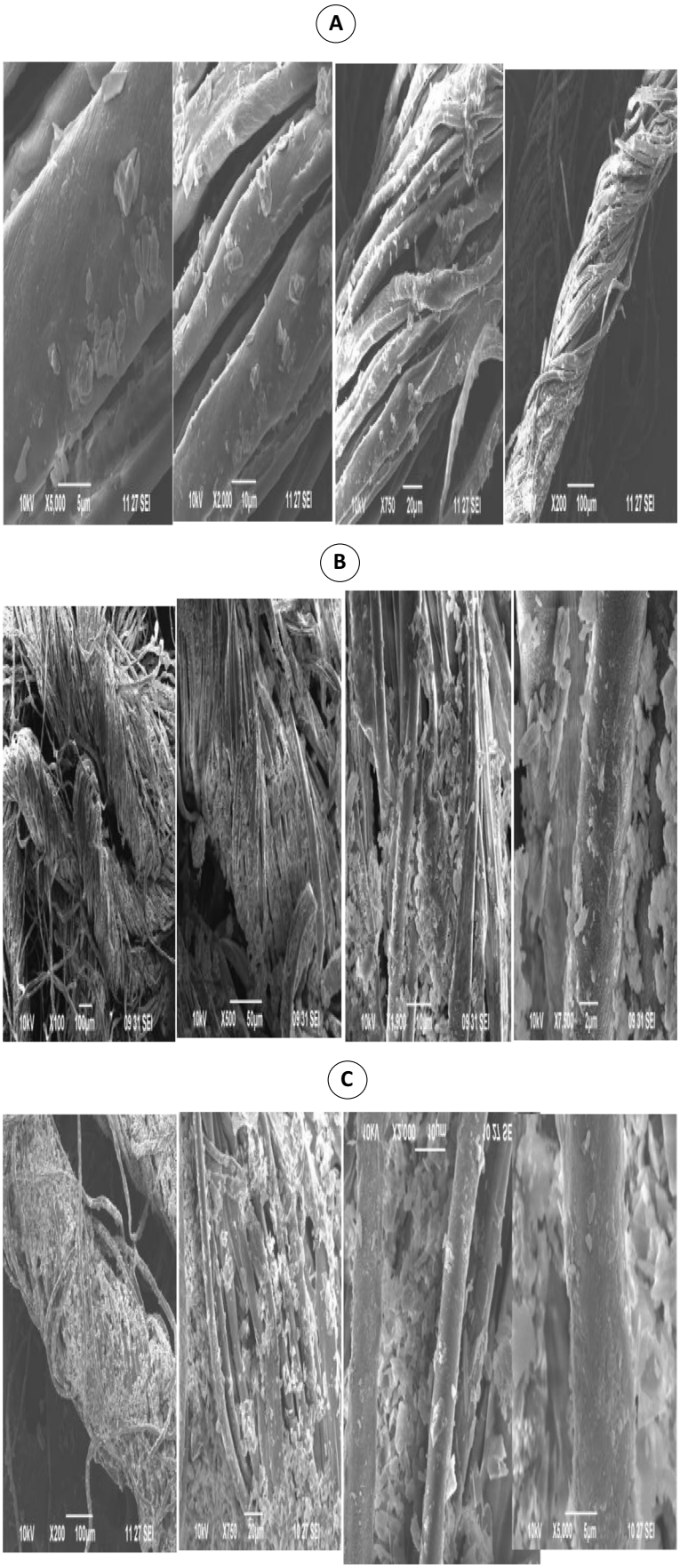

Fig. 6 SEM micrographs showing the images of hydroxyapatite nanoparticle which has crystal morphology developed by *Calotropis procera* (**B**), *Wrightia tinctoria* (**C**) plant latex serum extract and control (**A**)

Table 4 Antimicrobial activity of the developed hydroxyapatite nanoparticle shows zone of inhibition against the test pathogens

Test organism	Zone of inhibition (mm)		
	Control Hap Np	*C. procera* HAP Np	*W. tinctoria* Hap Np
Staphylococcus aureus	12 ± 0.8	22 ± 0.6	27 ± 0.7
Escherichia coli	09 ± 0.3	36 ± 0.8	34 ± 0.3
Aspergillus niger	10 ± 0.6	23 ± 0.2	25 ± 0.8
Candida albicans	07 ± 0.2	24 ± 0.5	24 ± 0.4

4 Conclusion

Cotton gauze natural properties were greatly improved by depositing nanoparticles (NP) on the surface as a suitable candidate for medical application as an advanced wound dress. The hydroxyapatite nanoparticles were successfully prepared using a *Calotropis procera* and *Wrightia tinctoria* latex serum extracts. The developed nanoparticles were characterized to determine the functional groups, lattice parameters, and crystal size and shape. Hence, the present manuscript suggests HAp NPs with plant latex serum extract were to imbue cotton gauze fabrics with antimicrobial activity. The latex serum of the plant has enormous bioactive compounds with a wide range of medicinal properties. The incorporation of HAp NPs with plant latex serum extract via wet chemical precipitation yielded the highest antimicrobial activities against various microorganisms (i.e., *Candida albicans*, *E. coli*, and *S. aureus*). The toxicity analysis revealed that the produced nanoparticle is non-toxic and can be recommended to the therapeutic purposes. The produced HAp Nps could be used as a promising material for wound healing in medical textiles which have good mechanical strength and possess the bioactivity. It is expected that the HAp Nps with plant extract is a promising and effective material to heal the bone fracture as potential bone implants in clinical applications.

Author contribution Authors 1 and 2 performed the experiment and implement the research. Author 3 performed the spectrum analysis. Author 4 contributed the final version of the draft. Author 5 substantially contributes to the design of the article and interpretation of the data.

Data availability All data generated and analyzed during this study are included in this article.

Declarations

Ethical approval Not applicable.

Competing interests The authors declare no competing interests.

References

1. Buzea C, Pacheco II, Robbie K (1992) Nanomaterials and nanoparticles: sources and toxicity. Biointerphases 2:17
2. DevanandVenkatasubbu G, Ramasamy S, Avadhani GS, Ramakrishnan V, Kumar J (2013) Surface modification and paclitaxel drug delivery of folic acid modified polyethylene glycol functionalized hydroxyapatite nanoparticles. Powder Technol 235:437–442
3. Dorozhkin SV (2010) Nanosized and nanocrystalline calcium orthophosphates. Acta Biomaterial 6:7–15
4. Govindan SK, Senkotuvel R, Sekar K, Raji G, Easwaradas KG, Gopalu K, Kuznetsov D (2017) Green synthesis and antibacterial activity of hydroyapatite nanorods for orthopedic applications. MRSCommunications 7:183–188
5. Kumar GS, Govindan R, Giriza EK (2014) In situ synthesis, characterization and in vitro studies of ciprofloxacin loaded hydroxyapatite nanoparticles for the treatment of osteomyelitis. J Mater Chem 2:50–52
6. Arsad MS, Lee PM, Hung LK (2011) Synthesis and Characterization of Hydroxyapatite Nanoparticles and β-TCP particles. Int Conf Biotechnol Food Sci 7:184–188
7. Mekala M, Sri MS, Suganya K (2019) Microencapsulation of Momordica cymbalaria (Athalakkai) fruit nanoparticle coated on cotton gauze for biomedical application. Aust J Basic Appl Sci 13(1):9–16
8. Hassan MH, Ismail MA, Moharram AM, Shoreit AA (2017) Phytochemical and antimicrobial of latex serum of *Calotropisprocera* and its silver nanoparticles against some reference pathogenic strains. J Ecol Health Environ 5(3):65–75
9. Okada M, Matsumoto T (2015) Synthesis and modification of apatite nanoparticles for use in dental and medical applications. Jpn Dent Sci Rev 51:85–95
10. Ramos MV, Aguiar VC, Melo VM, Mesquita RO, Silvestre PP, Oliveira JS (2007) Immunological and allergenic responses induced by latex fractions of *Calotropisprocera*. J Ethnopharmacol 111(1):115–122
11 Das RK, Babu PJ, Gogoi N, Sharma P, Bora U (2012) Microwave-mediated rapid synthesis of gold nanoparticles using *Calotropisprocera* latex and study of optical properties. ISRN Nanomaterials, pp 1–6
12. Rafie SMM, Nordin D (2017) Synthesis and characterization of hydtoyapatite nanoparticle. Malay J Anal Sci 21(1):136–148
13. Anuar A, Salimi MN, Daud MZ, Yee YF (2013) Characterizations of hydroxyapatite nanoparticles produced by sol-gel method. Adv Environ Biol 7(12):3587–3590
14. Utara S, Klinkaewnarong J (2016) Preparation of nano-hydroxyapatite particles by ultrasonic method at 25kHz using natural rubber latex as a templating agent. Chiang Mai J Sci 43(2):320–328
15. Suchanek W, Yoshimura M (1998) Processing and properties of hydroxyapatite based biomaterials for use as hard tissue replacement implants. J Mater Res 13:94
16. Suganya K, Atchaya P, Suba Sri M, Mekala M (2019) Hydroxyapatite herbal nanorods forbiomedical application. Int J Sci Res 8(8):1958–1962
17. Vedhanarayanan P, Unnikannan P, Sundaramoorthy P (2013) Antimicrobial activity and Phytochemical screening of *Wrightiatinctoria*. J Pharmacogn Phytochem 2(4):123–125
18. Balgova Z, Palou M, Wasserbauer J, Kozankova J (2013) Synthesis of poly(vinyl alcohol) - hydroxyapatite composites

and characterization of their bioactivity. Cent Eur J Chem 11(9):1403–1411
19. Alharbi NS, Alsubhi NS, Felimban AI (2022) Green synthesis of silver nanoparticles using medicinal plants: characterization and application. J Radiat Res Appl Sci 15(3):109–124
20. Ganta DD, Hirpaye BY, Raghavanpillai SK, Menber SY (2020) Green synthesis of hydroxyapatite nanoparticles using *Monoon longifolium* leaf extract for removal of fluoride from aqueous solution. J Chem 2020:4917604. https://doi.org/10.1155/2022/4917604
21 Mohamed NH, Ismail MA, Abdel-Mageed WM, Shoreit AA (2017) Biodegradation of natural rubber latex of *Calotropisprocera* by two endophytic fungal species. J Bioremediation Biodegradation 8(1):5
22 Lara-Ochoa S, Ortega-Lara W, Guerrero-Beltran CE (2021) Hydroxyapatite nanoparticles in drug delivery: physicochemical and applications. Pharmaceutics 13(10):1642
23. Wang Y, Tsuru K, Ishikawa K, Yokoi T, Kawashita M (2021) Fibronectin adsorption on carbonate containing hydroxyapatite. Ceram Int 47:11769–11776
24. Boukha Z, De Rivas B, Gonzalez-Velascoj R, Gutierrez-ortiz JI, Lopez- Fonseca R (2021) Comparative study of the efficiency of different noble metals supported on hydroxyapatite in the catalytic lean methane oxidation under realistic conditions. Materials 14:3612
25. Zandi M, Mirzadeh H, Mayer C, Urch H, Eslaminejad MB, Bagherif-Mivehchi H (2010) Biocompatibility evaluation of nanorod hydroxyapatite / gelatin coated with nano HAp as a novel scaffold using mesenchymal stem cells. J Biomed Mater Res 92:1244–1255

Publisher's note Springer Nature remains neutral with regard to jurisdictional claims in published maps and institutional affiliations.

Springer Nature or its licensor (e.g. a society or other partner) holds exclusive rights to this article under a publishing agreement with the author(s) or other rightsholder(s); author self-archiving of the accepted manuscript version of this article is solely governed by the terms of such publishing agreement and applicable law.